

Hall Effects on Unsteady Magnetohydrodynamic Flow of a Nanofluid Past an Oscillatory Vertical Rotating Flat Plate Embedded in Porous Media

M. Veera Krishna^{1,*}, N. Ameer Ahamad², and Ali J. Chamkha³

¹Department of Mathematics, Rayalaseema University, Kurnool 518007, Andhra Pradesh, India

²Department of Mathematics, Faculty of Science, University of Tabuk 71491, Kingdom of Saudi Arabia

³Faculty of Engineering, Kuwait College of Science and Technology, Doha District, 35004, Kuwait

In the current investigative paper, the impact of Hall current on an unsteady magnetohydrodynamic liberated convection revolving flow of a nanofluid restricted with a uniform absorbent medium over an oscillatory moving vertical smooth plate with convective as well as diffusive frontier conditions has been reviewed. The non-dimensionalized governing differential equations by the appropriate frontier conditions are resolved by the perturbations technique. The impacts of the physical constants on the flow as well as the heat transfer features are displayed graphically and analyzed for Cu as well as Al₂O₃ nanoparticles. For the engineering industry, the skin friction coefficient, local Nusselt number, along with the Sherwood's number are examined numerically in detail.

KEYWORDS: Chemical Reaction, Hall Effects, MHD, Nanofluid, Radiation Rotation.

IP: 95.175.65.65 On: Fri, 22 Oct 2021 05:45:38

Copyright: American Scientific Publishers

Delivered by Ingenta

1. INTRODUCTION

MHD convective heat transfer in nanofluids has many applications and participates in an essential task in both sciences and engineering. They need heat transfer fluids in technology for applications such as cooling or heating, solar energy, and nuclear reactors, among others. Since fluids have a lower thermal conductivity than metals, it is essential to combine all types of fluids with nano-sized metals to improve the fluids' heat transfer capacity. The deferment of nanoparticles inside a support fluid is referred to as a nanofluid.

Many authors¹⁻⁴ discussed the different type of nanofluids in various physical configurations. Ghalambaz and Noghrehabadi⁵ explored that the heat flux was increased for a case study of physical convection study over an upward plate-embedded nano-fluidized plate in a penetrable object that used a drift-flux pattern. Khairy et al.⁶ reviewed the barrier layer movement and heat transference moving a nonlinearly perforable flinching coat in a nanofluid. Abdelgaied and Mohamed⁷ discussed the mixed flow of nanofluid by a temperature-dependent viscosity nanofluid flow generated vertically, enclosed in a penetrable object with temperature subservient viscosity. Until

recently, the fluidity and non-linearity of natural MHD flows and particularly on unsteady magnetic structures were very sparsely studied by Loganathan et al.⁸ Das⁹ possessed the movement and heat transferal properties of nanofluids in a revolving frame. Ibrahim and Makinde¹⁰ developed a new method of discovering the MHD stagnation point and transporting temperature fluid through a flat region by applying the stretched thin Condensate nanofluids and slip-fluid convection. Das et al.¹¹ have gone into the dynamics of a magneto-fluid generated pore plate running flat inside a rotating container. Das et al.¹² scrutinised by a nanofluid barrier layer stream in a conical nozzle; the inlet temperature and outlet temperature varied following the applied hydraulic pressure, and standardized heat production was used as the means of heat exchange Chamkha and Aly¹³ examined, in the appearance of the engendering or consumption of MHD, the movement of a nanofluid over an upward plate due to free convection. Chamkha and Khaled¹⁴ investigated identity explications for MHD combined convicted heat and expanse variation in the penetrable material. Magyari and Chamkha¹⁵ also describe the thermo-solutal and boundary layers' details in exact numerical results. Khedr et al.¹⁶ demonstrated that MHD flow when applied pressure to a porous surface extended on the micro-Helenian-all-Hemotype. Chamkha et al.¹⁷ considered an unstable heat and expanse transference from a stretching exterior implanted in a liquid to a catalyst for this subject.

*Author to whom correspondence should be addressed.

Email: veerakrishna_maths@yahoo.com

Received: 1 April 2021

Accepted: 30 June 2021

In wholly the foregoing surveys, the Hall consequences are being disregarded. The attention of persistent fascinating terrain comprises the electro-magnetic forces together with Hall consequences might not be overlooked. As a matter of fact, Hall constraint is the proportion flanked by the cyclotron-electron periodicity and the atom-electron-collision prevalence. The Hall property is noteworthy while the magnetic scope is drugged or whilst the impingement incidence is near to the ground. Besides the ions along with electron-emissive encompass dissimilar accumulations by reason of which thyselves motions dispute. Customarily the electrons have superior dispersion velocity than with the intention of ions and as a primary proximity; dispersion speed of the electrons establishes the flow of charge compactness. While the electromagnetically forces are discernible, the dispersal velocity of the ions development is insignificant. As long as we believe the dispersal velocity of ions over and above such of electrons after that ions slip must not be overlooked. Hall possessions come across immense solicitations specifically when reviewed in conjunction with heat transport for instance refrigerator convolutes, MHD vulcanization accelerators, electrical charge manufacturers, etc. Krishna²² discovered the impacts of thermic transmission, Hall effects, and ion-sheet on the unstable MHD unconstrained convective spinning movement of Jeffrey liquid past an unbounded upright permeable plate ramped surface temperature. Krishna et al.²³ discovered the impacts of thermic transmission, Hall and ion slips impacts on the unstable MHD unconstrained convective spinning movement through a spongy media in a micro-outlet delimited by two never-ending upright equivalent plates owing to asymmetric heating. Krishna²⁴ sleuthing on the heat shipping for persistent MHD gush of Cu in addition to Al_2O_3 nanofluids across a elongation absorbent superficies. The compounded implications of Hall in addition ions slip about hydro magnetics pivoting flows of ciliary projection of diminutive architecture from end to end absorbent medium has discovered by Krishna et al.²⁵ Krishna²⁶ discussed the Hall along with ions slip special upshots going on hydro magnetics natural convectional revolving stream delimited through semi-countless perpendicular spongy facade. Krishna²⁷ addressed the MHD layered gush of galvanic performing Walter's liquid from beginning to end an annular cylinder or a conduit.

The thermal radiating, chemically reacting, Hall, and ions, slip consequences on coupled diffusive unstable MHD naturally revolving convection flows of micropolar liquid past a semi-unbounded an upward stirring spongy plate through convection boundary situations have been investigated with Krishna et al.²⁸ Krishna²⁹ investigated the radiation absorption, chemically reacted; Hall and ions slip implications on MHD warm convection wind past a semi tremendous stirring porous surface. Krishna in addition to Jyothi³⁰ discussed the impacts of temperature as well as

accumulation transport on liberated convection revolving stream of the viscoelastic fluid past a upright permeable plate by the time reliant fluctuatory penetrability as well as suction in occurrence of the consistent transversal magnetic domain as well as heat sources. Krishna as well as Reddy³¹ developed the transient hydro magnetic flows of a reacting second ordered fluids through the permeable media between two unlimitedly long flat analogous plates.

Keeping in mind the above, we reviewed warmth and mass transferal on an unstable MHD free convective rotating movement of a nanofluid past an oscillatory revolving an upward flat plate with convective and diffusive barrier circumstances in this article.

2. FORMULATION AND SOLUTION OF THE PROBLEM

It is contemplated unsteady MHD convective movement of an impenetrable nanofluid applied to a semi-incompressible an upward plate in a penetrable medium going through a continuous temperature gradient that has MHD buoyancy, and convective effects are passed overhead a horizontal plate interested in an immobile media in a vertically flowing medium amid a fluctuating electrically conducting flux. The mathematical design of the problem is as shown in the Figure 1. The flow is supposed to act in the x -path, this is exercised near the plate into the uphill inclination, and the axis of z is familiar to this. Furthermore, this was expected as the entire conformity is exchanging through the uniform velocity Ω about the z -path. A consistent surface magnetic domain B_0 is apprehended to be moving simultaneously on the z -axis. Both the fluid process the nanoparticles are thought to a state of thermic equanimity. It is assumed that no voltage is applied, implying the lack of an electric field.

Additionally, the influenced magnetic domain is thought to be weak in correlation to the outside magnetic environment. Due to the semi-unbounded plate exterior assuming, this means a low captivating Reynolds character for the revolving plate; additionally, the movement of variables

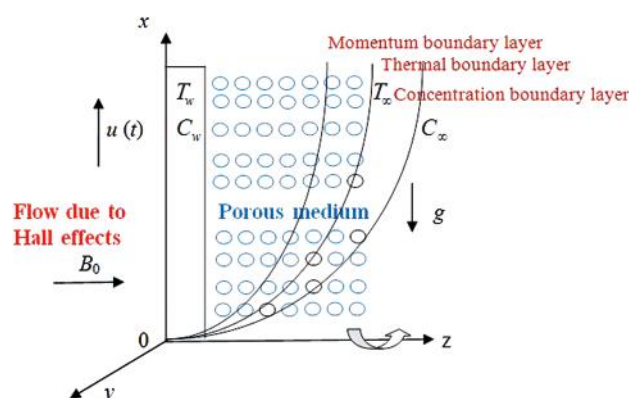


Fig. 1. Mechanical Configuration of the problem.

are parties of z and t exclusively. Das⁹ specifies the domain's leading problems.

$$\frac{\partial w}{\partial z} = 0 \tag{1}$$

$$\frac{\partial u}{\partial t} + w \frac{\partial u}{\partial z} - 2\Omega v = \frac{\mu_{nf}}{\rho_{nf}} \frac{\partial^2 u}{\partial z^2} + \frac{B_0 J_y}{\rho} - \frac{\mu_f}{k\rho_{nf}} u + g\beta_{nf}(T - T_\infty) + g\beta_{nf}^*(C - C_\infty) \tag{2}$$

$$\frac{\partial v}{\partial t} + w \frac{\partial v}{\partial z} + 2\Omega u = \frac{\mu_{nf}}{\rho_{nf}} \frac{\partial^2 v}{\partial z^2} - \frac{B_0 J_x}{\rho} - \frac{\mu_f}{k\rho_{nf}} v \tag{3}$$

$$\frac{\partial T}{\partial t} + w \frac{\partial T}{\partial z} = \alpha_{nf} \frac{\partial^2 T}{\partial z^2} + \frac{Q}{(\rho c_p)_{nf}} (T - T_\infty) - \frac{1}{(\rho c_p)_{nf}} \frac{\partial q_r}{\partial z} \tag{4}$$

$$\frac{\partial C}{\partial t} + w \frac{\partial C}{\partial z} = D_B \frac{\partial^2 C}{\partial z^2} + k_l(C - C_\infty) \tag{5}$$

Additionally, it is presumed that the plate surface heat is sustained through convection temperature transportation at the assured quantity T_w . Therefore, the boundary situations for the problem are specified as,

$$u = v = 0, \quad T = T_\infty, \quad C = C_\infty \quad \text{for } t \leq 0 \text{ and any } z \tag{6}$$

$$u = U_r \left(1 + \frac{\varepsilon}{2} (e^{int} + e^{-int}) \right), \quad v = 0, \tag{7}$$

$$-K_f \frac{\partial T}{\partial z} = h_f(T_w - T),$$

$$-D_B \frac{\partial C}{\partial z} = h_s(C_w - C), \quad \text{for } t > 0 \text{ and } z = 0$$

$$u = v = 0, \quad T \rightarrow T_\infty, \quad C \rightarrow C_\infty \quad \text{for } t > 0 \text{ and } z \rightarrow \infty \tag{8}$$

If the strengths of the magnetic domain are very huge, then the generalized Ohms commandment is adapted to includes the Hall impacts, therefore,

$$J + \frac{\omega_e \rho_e}{B_0} (J \times B) = \sigma_f \left(E + V \times B + \frac{1}{\rho_{ne}} \nabla p_e \right) \tag{9}$$

The ions slip as well as thermoelectric consequences are none incorporated. Additionally, the aforementioned is presumed that $\tau_e \omega_e \sim O(1)$ as well as $\omega_i \tau_i \leq 1$, here, ω_i as well as τ_i are the cyclotron frequencies as well as collisions time for ions, accordingly. In Eq. (9) be the electrons constraint gradients, the ions slip and thermoelectric impacts are none incorporated. It is also presumed the electric terminal $E = 0$. Under those presumptions reduced as,

$$J_x + m J_y = \sigma_f B_0 v \tag{10}$$

$$J_y - m J_x = -\sigma_f B_0 u \tag{11}$$

Where $m = \omega_e \tau_e$ the Hall current parameter. Solving Eqs. (10) and (11), it is obtained as,

$$J_x = \frac{\sigma_f B_0}{1 + m^2} (v + mu) \tag{12}$$

$$J_y = \frac{\sigma_f B_0}{1 + m^2} (mv - u) \tag{13}$$

Substitute the Eqs. (13)–(11) in Eqs. (2) and (3) accordingly, it is obtained as

$$\frac{\partial u}{\partial t} + w \frac{\partial u}{\partial z} + 2\Omega v = \frac{\mu_{nf}}{\rho_{nf}} \frac{\partial^2 u}{\partial z^2} + \frac{\sigma_{nf} B_0^2}{\rho(1 + m^2)} (mv - u) - \frac{\mu_f}{k\rho_{nf}} u + g\beta_{nf}(T - T_\infty) + g\beta_{nf}^*(C - C_\infty) \tag{14}$$

$$\frac{\partial v}{\partial t} + w \frac{\partial v}{\partial z} + 2\Omega u = \frac{\mu_{nf}}{\rho_{nf}} \frac{\partial^2 v}{\partial z^2} - \frac{\sigma_{nf} B_0^2}{\rho(1 + m^2)} (v + mu) - \frac{\mu_f}{k\rho_{nf}} v \tag{15}$$

The following table summarizes the properties of nanofluid.⁹ The adequate thickness of nanofluid is calculated as follows: $\sigma_{nf} = (1 - \phi)\rho_f + \phi\rho_s$, thermic diffusive of the nanofluids is $\alpha_{nf} = K_{nf}/(\rho c_p)_{nf}$, the density of nanofluid is yielded by $(\rho c_p)_{nf} = (1 - \phi)(\rho c_p)_f + \phi(\rho c_p)_s$, thermic conductivity regarding the nanofluid k_{nf} distinct aspects of nanoparticles, we fathered the resulting prescription, yielded by Hamilton and Crosser.¹⁸ $(k_{nf}/k_f) = ((k_s + (n_p - 1)k_s) - \phi(n_p - 1)(k_f - k_s)) / ((k_s + (n_p - 1)k_s) + \phi(k_f - k_s))$. The electrical conductivity of the nanofluid is provided by Das as well as Jana¹⁹ $\sigma_{nf} = \sigma_f (1 + ((3(\sigma - 1)\phi) / ((\sigma + 2) - (\sigma - 1)\phi)))$, $\sigma = \sigma_s / \sigma_f$, the thermic enlargement specification of the nanofluid is $(\rho\beta)_{nf} = (1 - \phi)(\rho\beta)_f + \phi(\rho\beta)_s$, the effective viscosity of the fluid is defined by an equation involving a dynamic viscosity variable $\mu_{nf} = \mu_f / (1 - \phi)^{2.5}$. Here, np denotes the form of the nanoparticle; for spherical formed nanoparticles, np equals 3, and for cylindrically shaped nanoparticles, np equals 3/2, The appendices nf , f , and s signify the nanofluid's thermodynamically attributes, primary fluid, and solid scraps, sequentially, and ϕ is abundant volume portion of nanoparticles.

Brewster²⁰ provides the radioactive heat definition using the Rosseland specification.

$$\frac{\partial q_r}{\partial z} = -16 \frac{T_\infty^3 \sigma^*}{3k^*} \frac{\partial^2 T}{\partial z^2} \tag{16}$$

It is introduced the subsequent non-dimensional masses are,

$$u^* = \frac{u}{U_r}, \quad v^* = \frac{v}{U_r}, \quad z' = \frac{z U_r}{\nu_f}, \quad t' = \frac{t U_r^2}{\nu_f} \tag{17}$$

$$n^* = \frac{n \nu_f}{U_r^2}, \quad \theta = \frac{(T - T_\infty)}{(T_w - T_\infty)}, \quad \psi = \frac{(C - C_\infty)}{(C_w - C_\infty)}$$

Making usage of a fore mentioned nanofluid characteristics of nanofluid, including by the Eqs. (16) as well as (17) in Eqs. (2) to (5), the following non dimensionalized equations (dropping asterisks)

$$J_1 \left(\frac{\partial u}{\partial t} - S \frac{\partial u}{\partial z} - Rv \right) = \frac{1}{(1-\phi)^{2.5}} \frac{\partial^2 u}{\partial z^2} + J_4 \frac{M^2(mv-u)}{1+m^2} - \frac{1}{K} u + J_2 \theta + J_3 L \psi \quad (18)$$

$$J_1 \left(\frac{\partial v}{\partial t} - S \frac{\partial v}{\partial z} - Ru \right) = \frac{1}{(1-\phi)^{2.5}} \frac{\partial^2 v}{\partial z^2} - J_4 \frac{M^2(v+mu)}{1+m^2} - \frac{1}{K} v \quad (19)$$

$$J_5 \left(\frac{\partial \theta}{\partial t} - S \frac{\partial \theta}{\partial z} \right) = \frac{N}{Pr} \frac{\partial^2 \theta}{\partial z^2} + Q_H \theta \quad (20)$$

$$\left(\frac{\partial \psi}{\partial t} - S \frac{\partial \psi}{\partial z} \right) = \frac{1}{Sc} \frac{\partial^2 \psi}{\partial z^2} + Kr \psi \quad (21)$$

Here, $R = (2\Omega v_f)/U_r^2$ is parameter of rotation, $S = w_0/U_r$ is the parameter of suction ($S > 0$) or ($S < 0$), $M = (\sigma_f B_0^2)/\rho_f U_r^2$ is the parameter of magnetic field, $K = (k U_r^2)/v_f^2$ is the permeability parameter, $Pr = \nu_f/\alpha_f$ is the Prandtl's quantity, $Q_H = (Q v_r^2)/(U_r^2 k_f)$ is the parameter of heat source, $Kr = (k_f v_f)/U_r^2$ is parameter of chemically reacting, $Sc = \nu_f/D_B$ is the Schmidt's quantity, $F = (4\sigma^* T_\infty^3)/(k_f k^*)$ is the parameter of thermic dissipation as well as $U_r = (g\beta_f(T_w - T_\infty))^{1/3}$ is velocity component.

As well, the frontier conditions (6)–(8) reduced to,

$$u = v = 0, \quad \theta = 0, \quad \psi = 0 \quad \text{for } t \leq 0 \text{ and any } z \quad (22)$$

$$u = U_r \left(1 + \frac{\varepsilon}{2} (e^{int} + e^{-int}) \right), \quad v = 0, \\ \theta'(z) = -N_c (1 - \theta(z)), \\ \psi' = -N_d (1 - \psi(z)) \quad \text{for } t > 0 \text{ and } z = 0 \quad (23)$$

$$u = v = 0, \quad \theta \rightarrow 0, \quad \psi \rightarrow 0 \quad \text{for } t > 0 \text{ and } z \rightarrow \infty \quad (24)$$

Where, $N_c = (h_f v_f)/(K_f U_r)$ is the specification of convective and $N_d = (h_s v_f)/(D_B U_r)$ is the specification of diffusive. Combining Eqs. (18) and (19), Let $q = u + iv$ and it is collected as,

$$J_1 \left(\frac{\partial q}{\partial t} - S \frac{\partial q}{\partial z} - iRq \right) = \frac{1}{(1-\phi)^{2.5}} \frac{\partial^2 q}{\partial z^2} - \left(J_4 \frac{M^2}{1-im} + \frac{1}{K} \right) q - J_2 \theta + J_3 L \psi \quad (25)$$

The subsequent frontier conditions become

$$q = 0, \quad \theta = 0, \quad \psi = 0 \quad \text{for } t \leq 0 \text{ and any } z \quad (26)$$

$$q = U_r \left(1 + \frac{\varepsilon}{2} (e^{int} + e^{-int}) \right), \\ \theta'(z) = -N_c (1 - \theta(z)), \\ \psi' = -N_d (1 - \psi(z)) \quad \text{for } t > 0 \text{ and } z = 0 \quad (27)$$

$$q = 0, \quad \theta \rightarrow 0, \quad \psi \rightarrow 0 \quad \text{for } t > 0 \text{ and } z \rightarrow \infty \quad (28)$$

It is obtained the solutions of the scheme of partial differential Eqs. (20), (21) as well as (25) under the frontier conditions characterized in (26) to (28), it is expressed, velocity, temperature as well as concentration as.²¹

$$q(z, t) = q_0 + \frac{\varepsilon}{2} (e^{int} q_1(z) + e^{-int} q_2(z)) \quad (29)$$

$$\theta(z, t) = \theta_0 + \frac{\varepsilon}{2} (e^{int} \theta_1(z) + e^{-int} \theta_2(z)) \quad (30)$$

$$\psi(z, t) = \psi_0 + \frac{\varepsilon}{2} (e^{int} \psi_1(z) + e^{-int} \psi_2(z)) \quad (31)$$

Substituted the fore mentioned Eqs. (29), (30) as well as (31) into the Eqs. (20), (21) as well as (25), in addition to equating the harmonic along with non-harmonic terms as well as ignoring the highest ordered expressions of ε^2 , it is obtained following equations,

$$A \frac{d^2 q_0}{dz^2} + J_1 S \frac{dq_0}{dz} + (iR J_1 - B) q_0 + J_2 \theta_0 + J_3 \psi_0 L = 0 \quad (32)$$

$$N \frac{d^2 \theta_0}{dz^2} + Pr S J_5 \frac{d\theta_0}{dz} + Q_H \theta_0 = 0 \quad (33)$$

$$\frac{d^2 \psi_0}{dz^2} + S Sc \frac{d\psi_0}{dz} + Kr Sc \psi_0 = 0 \quad (34)$$

The first order equations are:

$$A \frac{d^2 q_1}{dz^2} + J_1 S \frac{dq_1}{dz} + (iJ_1(R-n) - B) q_1 + J_2 \theta_1 + J_3 \psi_1 = 0 \quad (35)$$

$$N \frac{d^2 \theta_1}{dz^2} + Pr J_5 S \frac{d\theta_1}{dz} + (Q_H - Pr J_5 in) \theta_1 = 0 \quad (36)$$

$$\frac{d^2 \psi_1}{dz^2} + S Sc \frac{d\psi_1}{dz} + Sc(Kr - in) \psi_1 = 0 \quad (37)$$

The second order equations are:

$$A \frac{d^2 q_2}{dz^2} + J_1 S \frac{dq_2}{dz} + (iJ_1(R+n) - B) q_2 + J_2 \theta_2 + J_3 L \psi_2 = 0 \quad (38)$$

$$N \frac{d^2 \theta_2}{dz^2} + Pr S J_5 \frac{d\theta_2}{dz} + (Q_H + Pr J_5 in) \theta_2 = 0 \quad (39)$$

$$\frac{d^2 \psi_2}{dz^2} + S Sc \frac{d\psi_2}{dz} + Sc(Kr + in) \psi_2 = 0 \quad (40)$$

The corresponding boundary conditions are,

$$\begin{aligned}
 q_0 = q_1 = q_2 = 1; \quad \frac{d\theta_0}{dz} &= -N_c(1 - \theta_0), \\
 \frac{d\theta_1}{dz} &= N_c\theta_1, \quad \frac{d\theta_2}{dz} = N_c\theta_2 \\
 \frac{d\psi_0}{dz} &= -N_d(1 - \psi_0), \quad \frac{d\psi_1}{dz} = N_d\psi_1, \\
 \frac{d\psi_2}{dz} &= N_d\psi_2; \quad \text{at } z=0
 \end{aligned} \tag{41}$$

$$\begin{aligned}
 q_0, q_1, q_2 \rightarrow 0; \quad \theta_0, \theta_1, \theta_2 \rightarrow 0; \\
 \psi_0, \psi_1, \psi_2 \rightarrow 0, \quad \text{at } z \rightarrow \infty
 \end{aligned} \tag{42}$$

Solving the equations from (32)–(40) under the boundary conditions (34) as well as (35), it is obtained the zeroth, first ordered as well as second ordered solutions. Now substitution of these in Eqs. (29)–(31), gave the equations for velocity, temperatures as well as concentrations distributions as followed by,

$$\begin{aligned}
 q &= (1 - A_1 - A_2)e^{-m_3z} + A_1e^{-m_1z} + A_2e^{-m_2z} \\
 &+ \frac{\varepsilon}{2}(e^{-m_4z}e^{int} + e^{-m_5z}e^{-int})
 \end{aligned} \tag{43}$$

$$\theta = B_2e^{-m_2z} \tag{44}$$

$$\psi = B_1e^{-m_1z} \tag{45}$$

For the scope of industrial engineering innovations, the confined skin frictions coefficients C_f , confined Nusselt number Nu_x as well as confined Sherwood number Sh_x were specified through,

$$\begin{aligned}
 C_f &= \frac{\tau_w}{\rho_f U_w^2}, \quad Nu_x = \frac{xq_w}{k_f(T_w - T_\infty)} \\
 \text{and } Sh_x &= \frac{xq_m}{D_B(C_w - C_\infty)}
 \end{aligned} \tag{46}$$

Here, the wall shear stress τ_w is specified through $\tau_w = \mu_{nf}(\partial q/\partial z)_{z=0}$.

The wall heat discharge is specified through $q_w = -k_{nf}(\partial\theta/\partial z)_{z=0}$.

The wall mass discharge is specified through $q_m = -\mu_{nf}(\partial\phi/\partial z)_{z=0}$.

$$\begin{aligned}
 C_f &= -A \left((1 - A_1 - A_2)m_3 + A_1m_1 + A_2m_2 \right. \\
 &\left. + \frac{\varepsilon}{2}(m_4e^{int} + m_5e^{-int}) \right)
 \end{aligned} \tag{47}$$

$$Nu_x = \frac{k_{nf}}{k_f} B_2 m_2 \tag{48}$$

$$Sh_x = B_1 m_1 \tag{49}$$

3. RESULTS AND DISCUSSION

The flow dictated by the non dimensionalized specifications, specifically viz. the specification of Hartmann M , the specification of rotations R , the specification of volume fractions of nanoparticles ϕ , nanoparticle shape n_p , the specification of convective N_c , the specification of diffusive N_d , the specification of suction S , the specification of radiation F , the specification of heat source Q_H and the specification of chemical reacting Kr on velocity, temperatures and concentrations distributions; also skin frictions, local Nusselt number as well as Sherwood number. For computational purpose, these are fixing $Pr=6.72$, $n_p=3$, $t=1$ and $n=\pi/3$. Figures 2–9, 10(a)–(e) and 11(a)–(d) represented the velocity, temperature as well as concentration delivery with esteem to the leading parameters. The thermophysical characteristics of water (support fluid), Cu (copper) as well as Al_2O_3 (Alumina) are given into Table I.

We noticed from the Figure 2 that an enhancement in the Hartmann specification M deflates the velocity sketches for u as well as v of the flows of both Cu-water in addition to Al_2O_3 -water nanoliquids. The reinforcing in the captivating field inferences to increase the reverse force to the flows is known as ‘‘Lorentz force.’’ The magnetic field impact is highest momentous on copper-water nanoliquid, whereas compared with the Al_2O_3 -water nanoliquid.

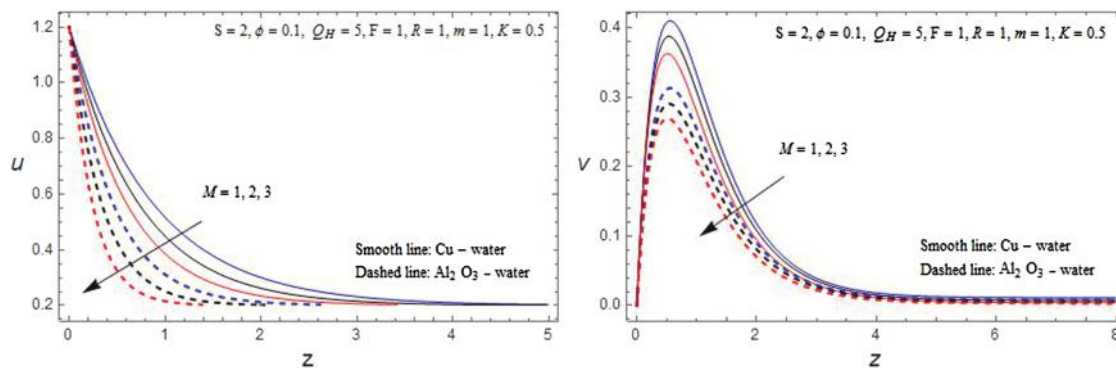
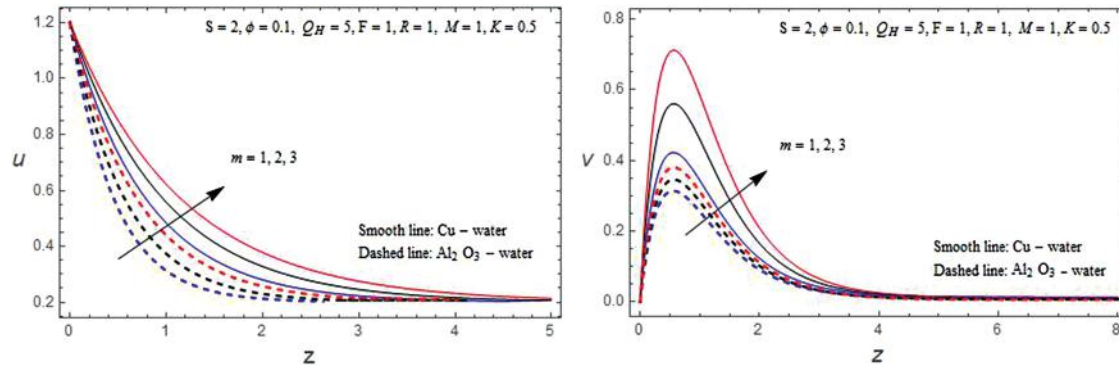
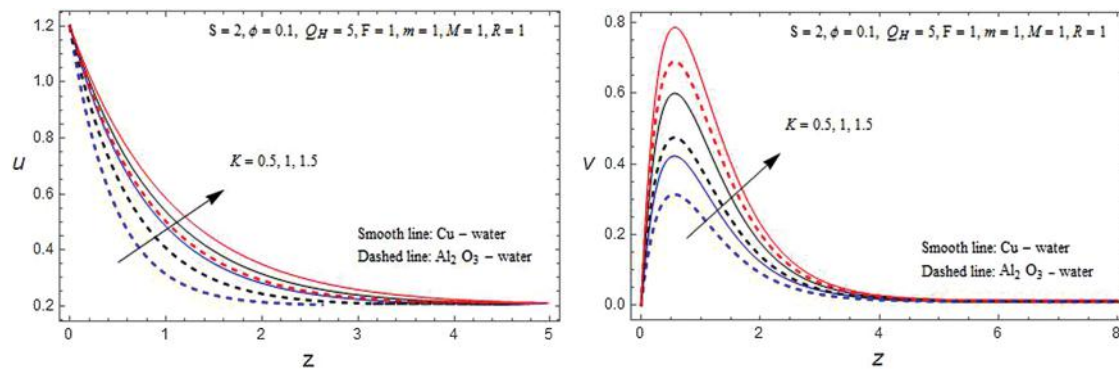
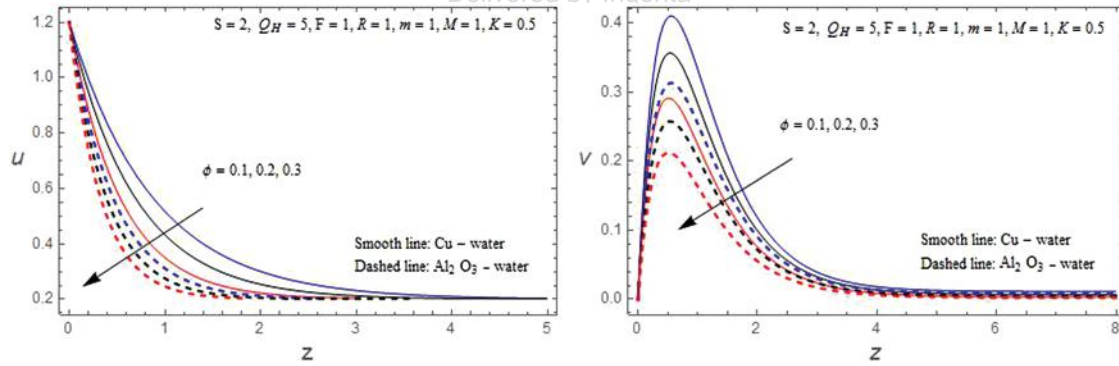
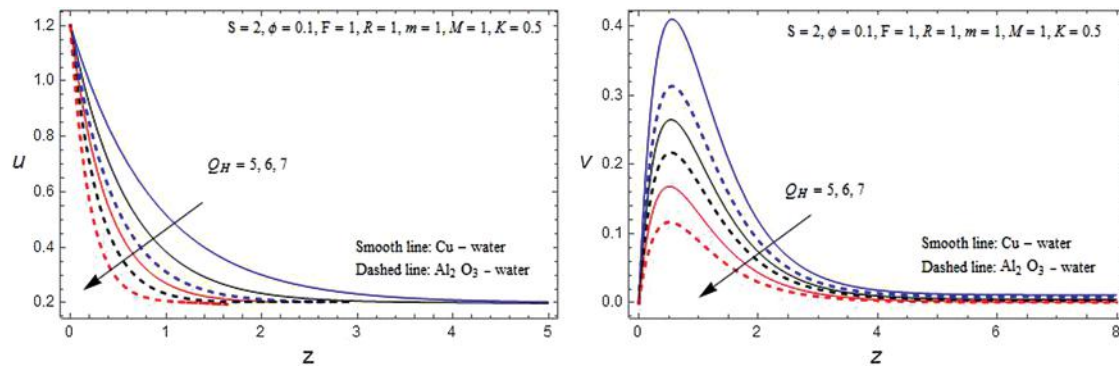


Fig. 2. Profiles of u and v with M .

Fig. 3. Profiles of u and v with m .Fig. 4. Profiles of u and v with K .Fig. 5. Profiles of u and v with ϕ .Fig. 6. Profiles of u and v with Q_H .

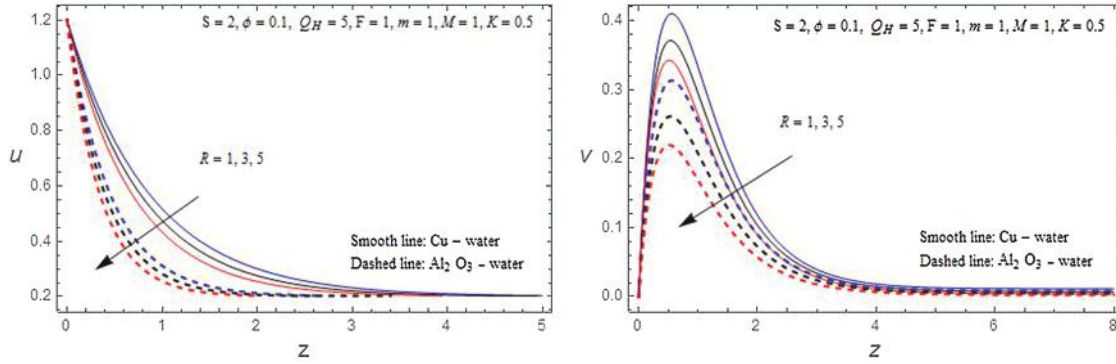


Fig. 7. Profiles of u and v with R .

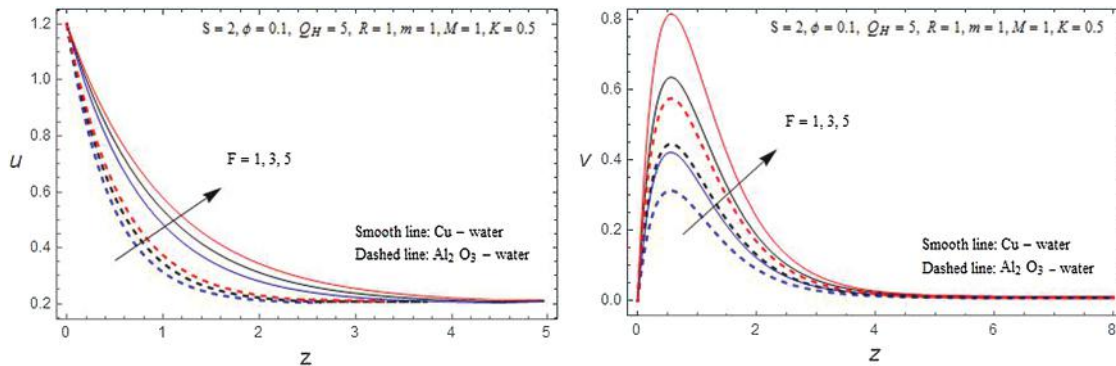


Fig. 8. Profiles of u and v with F .

The outcome velocity is also diminished with enhancing in the strength of the captivating field. The Figures 3–4 depicted the impacts of Hall currents and permeability of the penetrable medium on velocity outlines of u and v . The magnitudes of the velocity constituents for u as well as v improve with an enhancing in Hall specification m and the penetrable specification K . The outcome velocity is also boost up with enhancing either m or K for together copper–water as well as Al_2O_3 –water nanofluids. Lesser the penetrability lower the fluid velocity is noticed in the complete liquid regions. Figure 5 illustrate the impact of nanoparticle capacity fractions ϕ on velocity outlines for

u as well as v . This is cleared that by an increasing in volume fractions of the nanoparticle diminishes the velocity together Cu-water as well as Al_2O_3 -water nanofluids. This is owing to the piece of evidence that an increasing in the volume fractions develops the density of the nanofluid as well as it reasons to decelerate the liquid velocity. We noticed that the velocity constituents for u as well as v reduce with an accession in heat origin specification Q_H and rotation parameter R (Figs. 6–7). An increment in the heat generation or absorptions specification declines the velocity contours. Due to the domination of the temperature absorptions coefficient, it is expressed that, lessening

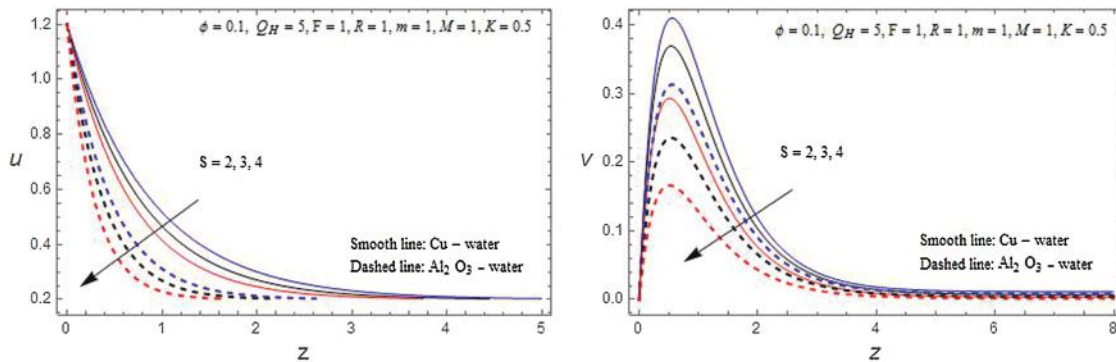


Fig. 9. Profiles of u and v with S .

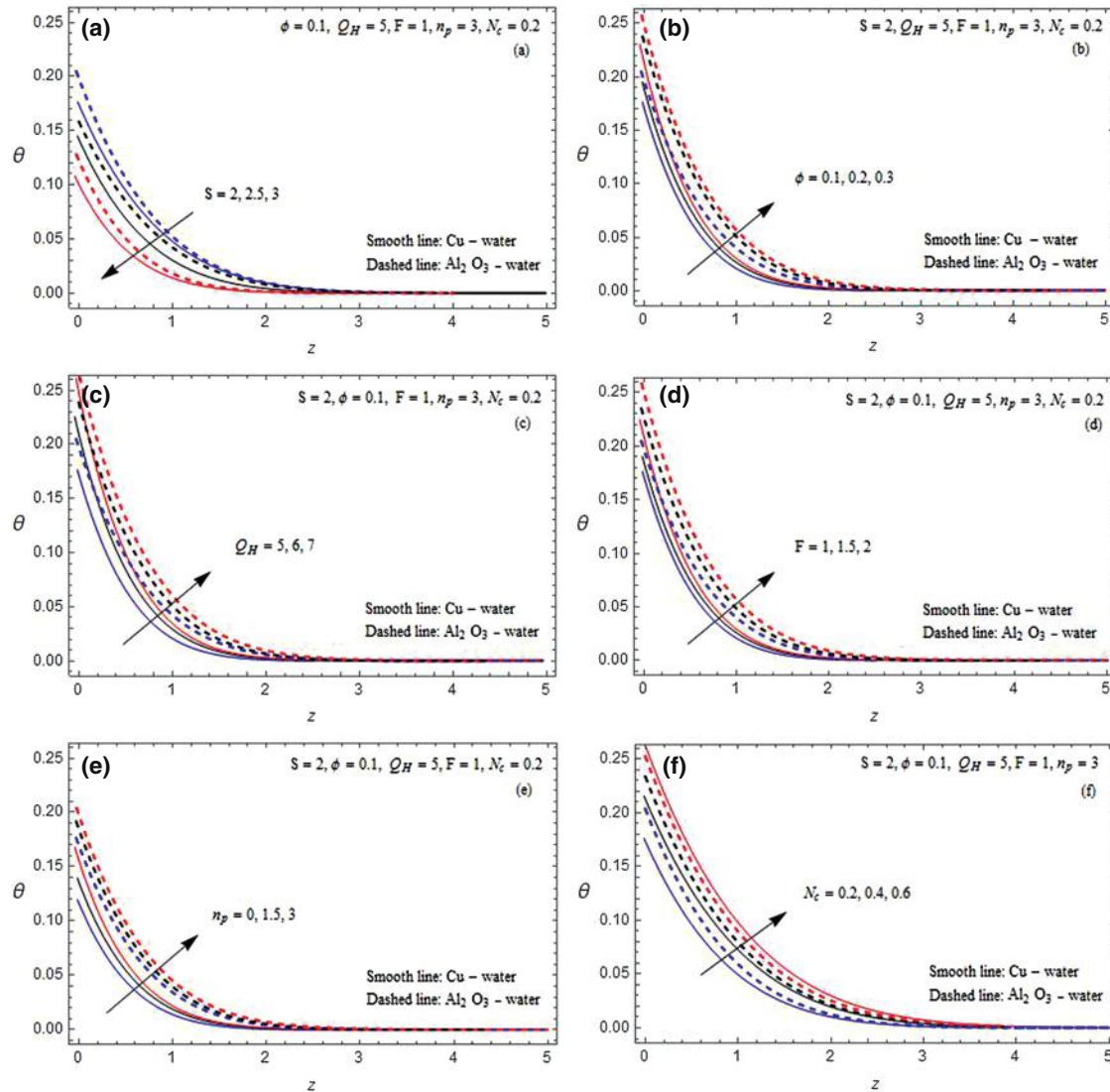


Fig. 10. (a-f) The temperature with S , ϕ , Q_H , F , n_p and N_c .

in the velocity specifications u and v . At the same time, when the revolution enhances progressively then velocity of the liquid follows the frontier as well as this is ignorable far gone from the frontier. Hence the resulting velocity reduces with an enhancing in ϕ , Q_H and R . Figure 8 illustrates the radiation impact on velocity profiles for u as well as v . This is scrutinized that an increment in the radiating parameters boost up the velocity profiles for u as well as v of the move domain. An increment in radioactivity liberates the heat to flow, magnifying the impulse barrier layer density. Figure 9 displays the magnetism of the suction specification on velocity specifications u as well as v of the flow. This was commented that an improvement in the suction specification turns down the energy barrier layer. The suction sustains the completion of the frontier layer. It has told that the expected physical nature of the power specification S .

The suction specifications effect on the flow's temperature outlines is depicted in Figure 10(a). Increases in the suction parameter result in a depreciation of the thermal boundary sheet. This may be because suction acts as a stabilizer for the barrier layer's formation. This is compatible with the suction parameter's ordinary physical existence. This is cleared that from Figure 10(b), for an improvement in the amount of nanoparticle concentration grows the temperature silhouettes of together Cu-water as well as Al_2O_3 -water nanofluids. This is because increasing the amplification portion increases the frequency of the nanofluid, which results in an improvement in thermic potential. It is exciting to transcribe that Cu-limewater nanofluid has adequate thermic potential while connected with Al_2O_3 -water nanofluid. It is evident from the Figure 10(c) fact that the temperature enhances with improving Heat source specification Q_H .

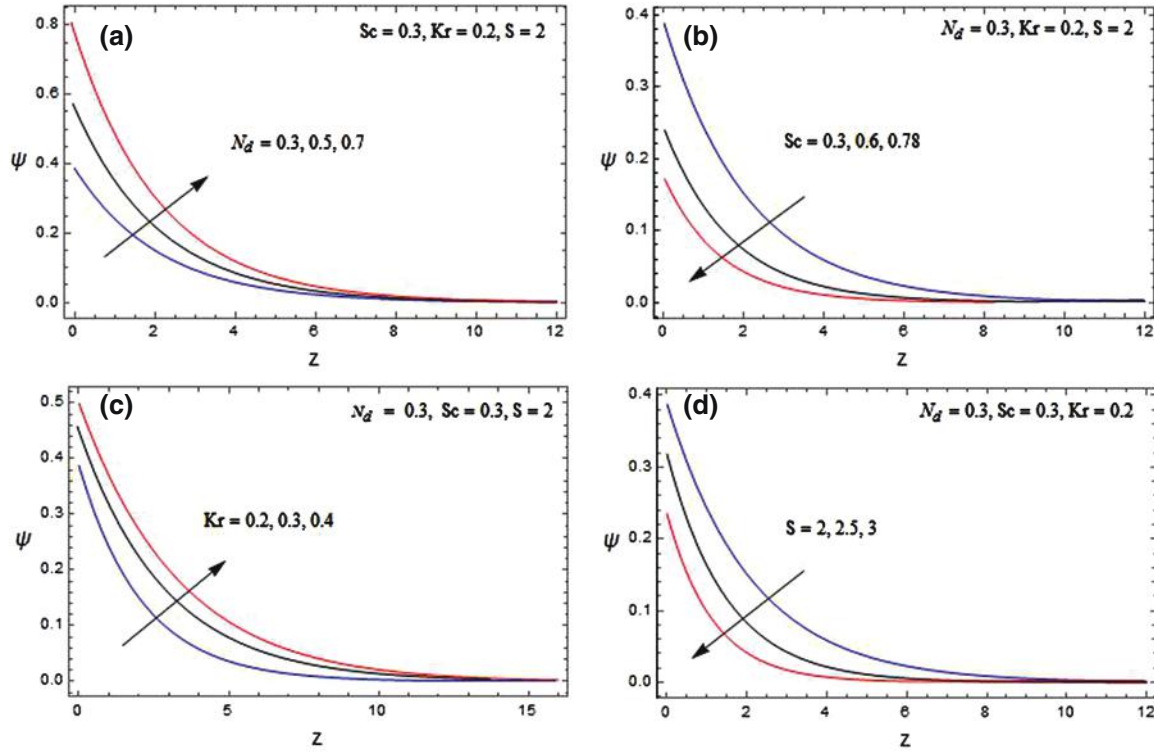


Fig. 11. (a–d) Concentration with N_d , Sc , Kr and S .

IP: 95.175.65.65 On: Fri, 22 Oct 2021 05:45:38
 Copyright: American Scientific Publishers

Table I. Thermophysical characteristics of water, Copper and Alumina.

Thermophysical properties	Base fluid (Water)	Cu (Copper)	Al ₂ O ₃ (Alumina)
c_p (J/Kg K)	4179.0	0385	0765
ρ (Kg/m ³)	997.14	8933.3	3950
K (W/m K)	0.6132	0040	0040
$\beta \times 10^{-5}$ (1/K)	0021	1.6701	0.850

Figure 10(d) illustrates respectively, the radiation influence temperature silhouettes. It is found that increasing the radiation specification improves the flow's temperature profiles. Physically, a rise in radiation transfers heat to the flow, contributing to the thicknesses of the thermally border stratum. Figure 10(e) illustrates the influences of the shapes of the nanoparticle on the temperature distribution. We discovered an intriguing result: the nanoparticles'

Table II. Skin friction (C_f).

M	m	K	ϕ	R	F	Q_H	S	Cu–H ₂ O	Al ₂ O ₃ –H ₂ O
1.0	1.0	0.5	0.1	1.0	1.0	5.0	2.0	0.6552582	0.7885952
2.0								0.8599601	0.9669853
3.0								0.9544783	1.2445811
	2.0							0.4885792	0.6201452
	3.0							0.3458781	0.4701413
		1.0						0.5200124	0.6995892
		2.0						0.4125583	0.5887494
			0.2					0.7445121	0.8859223
			0.3					0.9966362	0.9988772
				3.0				0.3225623	0.5662581
				5.0				0.1555244	0.3366253
					3.0			0.7088591	0.9966582
					5.0			0.9112452	1.1885411
						6.0		0.8221453	0.8884744
						7.0		1.0025221	1.1145281
							3.0	0.5221462	0.6699802
							4.0	0.3558963	0.5411553

Table III. Nusselt number (Nu_x).

N_c	F	Q_H	ϕ	n_p	S	Cu-H ₂ O	Al ₂ O ₃ -H ₂ O
0.2	1.0	5.0	0.1	3.0	2.0	0.214452	0.204458
0.4						0.287885	0.288595
0.6						0.356558	0.366658
	1.5					0.284789	0.345889
	2.0					0.378012	0.452216
		6.0				0.154152	0.152245
		7.0				0.122198	0.114588
			0.2			0.285479	0.289960
			0.3			0.336256	0.399901
				0.0		0.285545	0.252214
				1.5		0.250014	0.235589
					3.0	0.114552	0.189663
					4.0	0.045585	0.144785

Table IV. Sherwood number (Sh_x).

N_d	Kr	Sc	S	Sh_x
0.30	0.20	0.22	2.00	0.1465034
0.50				0.1820683
0.70				0.2032104
	0.50			0.1590364
	0.80			0.1824823
		0.30		0.1836012
		0.60		0.2352471
			2.50	0.1804522
			3.00	0.1982771

spherical structure contributes to a steady increase in temperature. We conclude that, compared to cylindrical-shaped nanoparticles, spherical-shaped nanoparticles allow more effectively heat conductance of the flow. The influence of the convective specification N_c on temperature is expressed in Figure 10(f). An expanding in N_c increases the temperature outlines. In general, the N_c have a leaning to intensify the thermic barrier thickness, and this prompts to improve the heat transference rate.

The suction parameter, Schmidt number, chemically reacted, and diffusion specifications of all impact the concentration outlines of the flow domain in Figures 11(a)–(d). As shown in the figures, increasing the

suction parameter or Schmidt specification decreases the flow's concentration outlines. Expanding the chemically reaction or diffusion parameter increases the concentration in the fluid area. Tables II–IV designate the specifications of skin frictions, Nusselt number, as well as Sherwood number representations concerning the governing specifications. An increase in Hall parameters m , penetrable parameters K , revolving parameters R , as well as suction variable S reduces the skin frictions. As well these enhance by an enhancing in the Hartmann parameter M , volume fractions parameter ϕ , radiation parameter F as well as heat source parameter Q_H (Table II). As of Table III, it is possessed that, Nusselt number Nu increase with an enhancing in convective parameter N_c , radiating parameter F as well as volume fractions parameter ϕ , in addition, this is reduced with an enhancing in heat source parameter Q_H , nanoparticle shape n_p and suction parameter S . Finally, as of Table IV, this was noticed that, the Sherwood number Sh increases with an enhancing in every one parameter diffusion parameter N_d , chemical-reaction parameter Kr , Schmidt number Sc as well as suction parameter S . Table V displayed that, the comparisons of the current outcomes by the previous outcomes of Das.⁹ It is found excellent conformity of the current outcomes with the previous outcomes.

Table V. Comparisons of Outcomes ($F=Kr=Sc=m=0$).

M	ϕ	R	C_f Das ⁹	C_f current results	Nu_x/Re_x Das ⁹	Nu_x/Re_x present results
1	0.1	1	2.145221	2.145255	0.521452	0.521455
2			1.855472	1.855485	0.485596	0.485599
3			1.655212	1.655222	0.445201	0.445204
4			1.458854	1.458868	0.401152	0.401158
	0.2		2.336650	2.336665	0.552468	0.552472
	0.3		2.666325	2.666335	0.589985	0.589988
	0.4		3.014452	3.014467	0.610225	0.610228
		3	2.544481	2.544855	0.524252	0.524255
		5	2.880112	2.880411	0.528854	0.528856
		8	3.184475	3.184486	0.529960	0.529962

4. CONCLUSIONS

It is deemed the Hall current impacts on an unstable liberated convection revolving flow of the nanofluid bounded by the uniform absorbent media past the oscillatory unbounded moving vertical flat plate with convective as well as diffusive boundary conditions. The results are abridged as follows. The radiation parameter in addition to Hartmann number have propensity to diminish the outcomes velocity. The outcomes velocity enhanced by an increasing in Hall current specification. The convection specification helps to intensify the temperature diffusion. Concentration diminishes with enhancing suction specification. The specification Radiation and nanoparticle volume fractions increase the rate of temperature transportation. The suction parameter facilitates to increase the rates of mass transport at the boundary.

Conflicts of Interests

The authors declare no conflicts of interest.

Acknowledgments: The authors are very much thankful to Department of Mathematics, Rayalaseema University, Kurnool, India, providing high performance software for computational work of this paper.

References and Notes

1. M. Sheikholeslami, H. R. Ashorynejad, G. Domairry, and I. Hashim, *Journal of Applied Mathematics* 2012, 421320 (2012).
2. A. T. Baheta and A. D. Woldeyohannes, *Asian Journal of Scientific Research* 6, 339 (2013).
3. E. V. Timofeeva, J. L. Routbort, and D. Singh, *J. Appl. Phys.* 106, 014304 (2009).
4. R. N. Barik, G. C. Dash, and M. Kar, *Journal of Applied Analysis and Computation* 4, 231 (2014).
5. M. Ghalambaz and A. Noghrehabadi, *Journal of Computational Applied Research in Mechanical Engineering* 3, 113 (2014).
6. Z. Khairy, A. Ishak, and I. Pop, *Science Reports* 4, 4404 (2014).
7. S. M. Abdelgaied and R. E. Mohamed, *Recent Adv. Math. Methods Comput. Tech. Mod. Ser.* 3, 300 (2013).
8. P. Loganathan, C. P. Nirmala, and P. Ganesan, *Thermal Science* 19, 1037 (2015).
9. K. Das, *Alexandria Engineering Journal* 53, 757 (2014).
10. W. Ibrahim and O. D. Makinde, *Journal of Aerospace Engineering* 11, 04015037 (2015).
11. S. Das, H. K. Mandal, R. N. Jana, and O. D. Makinde, *J. Nanofluids* 4, 167 (2015).
12. S. Das, R. N. Jana, and O. D. Makinde, *International Journal of Nano Science* 13, 1450019 (2014).
13. A. J. Chamkha and A. M. Aly, *Chem. Eng. Commun.* 198, 425 (2011).
14. A. J. Chamkha and A. R. A. Khaled, *International Journal of Numerical Methods for Heat and Fluid Flow* 10, 94 (2000).
15. E. Magyari and A. J. Chamkha, *International Journal of Thermal Science* 47, 848 (2008).
16. M. E. M. Khedr, A. J. Chamkha, and M. Bayomi, *Nonlinear Analysis: Modeling and Control* 14, 27 (2009).
17. A. J. Chamkha, A. M. Aly, and M. A. Mansour, *Chem. Eng. Commun.* 197, 846 (2010).
18. R. L. Hamilton and O. K. Crosser, *J. Ind. Eng. Chem. Fund.* 1, 187 (1962).
19. S. Das and R. N. Jana, *Alexandria Engineering Journal* 54, 55 (2015).
20. M. Q. Brewster, *Thermal Radiative Transfer and Properties*. John Wiley & Sons, United States (1992).
21. R. Ganapathy, *Journal of Applied Mechanics* 61, 205 (1994).
22. M. V. Krishna, *International Communications in Heat and Mass Transfer* 119, 104927 (2020).
23. P. M. S. Basha, M. V. Krishna, and N. Nagarathna, *Heat Transfer* 45, 4264 (2020).
24. M. V. Krishna, *Heat Transfer* 49, 1374 (2020).
25. M. V. Krishna, C. S. Sravanthi, and R. S. R. Gorla, *International Communications in Heat and Mass Transfer* 112, 104500 (2020).
26. M. V. Krishna, *Heat Transfer* 49, 2020 (2020).
27. M. V. Krishna, *Heat Transfer* 49, 2311 (2020).
28. M. V. Krishna, N. A. Ahamad, and A. F. Aljohani, *Alexandria Engineering Journal* 60, 3467 (2021).
29. M. V. Krishna, *Chin. J. Chem. Eng.* 31, 1 (2021).
30. M. V. Krishna and K. Jyothi, *J. Anal.* 27, 643 (2019).
31. M. Krishna and G. S. Reddy, *J. Anal.* 27, 103 (2019).